Available online at www.sciencedirect.com
ScienceDirect
Polymer 48 (2007) 3759–3770
polymer
www.elsevier.com/locate/polymer

Hierarchical self-assembling of dendritic–linear diblock complex based on hydrogen bonding

Qingtao Liu [a], Hui Zhang [a], Shengyan Yin [a], Lixin Wu [a,*], Chen Shao [b], Zhongmin Su [b]

[a] *Key Laboratory for Supramolecular Structure and Materials of Ministry of Education, Jilin University, Qianjin Street 2699, Changchun 130012, PR China*
[b] *College of Chemistry, Northeast Normal University, Changchun 130022, PR China*

Received 13 February 2007; received in revised form 11 April 2007; accepted 13 April 2007
Available online 4 May 2007

Abstract

An effective route was demonstrated to fabricate vesicles, cylindrical micelles, fibers and hierarchical structures by using dendritic–linear amphiphilic diblock complex as building block through hydrogen bonding. We tailored the formation and evolution of these aggregation morphologies as well as the transformation among them, and found that the concentration and solvent polarity could affect the aggregation states of the complex in solution and the self-assembling process on solid substrate. Additionally, the flexible-rigid structure of the complex and the template effect of DMSO droplets resulting from solvent evaporation also play important roles in constructing higher level organized structures such as hierarchical wreath-like and hollow entanglement self-assemblies at solid–gas interface. The cast film of the complex which possesses a fibrous structure shows superhydrophobicity and when the solution was allowed to stand for some days, a transparent organic gel spontaneously formed from the mixed solution. Based on the experiment results, the hierarchical architectures are proposed to derive from primary fibrils. The structure of the cylindrical micelle is believed to possess an alkyl chain block shell and a poly(ethylene oxide) block core, which is consistent with the water contact angle measurement and the simulation to the volume ratio of the two blocks of the complex.

Keywords: Supramolecular chemistry; Hierarchical self-assemble; Hydrogen bonding

1. Introduction

Supramolecular self-assembling has attracted considerable attention over recent years because it provides a method for spontaneous generation of well-defined architectures through non-covalent interactions such as electrostatic, hydrogen bonding, π–π, dipole–dipole and van der Waals interaction [1–3]. Various precisely designed building blocks such as low-weight molecules, macromolecules and complexes have been applied for the purpose, and many interesting self-assembled structures such as globular, lamellar and cylindrical micelles, fibers, nanorods and nanotubes as well as hollow vesicles have been created [4–9]. Thus the construction of ordered aggregation structures and the controllable transformation between aggregated morphologies display their significance in organized solution systems [10]. Very recently, hierarchical self-assembling becomes a challenging topic in chemistry and materials, especially in the aspects of dealing with understanding the nature of bio-structure and constructing more complicated multifunctional nanomaterials and devices [11–13]. Diverse effective methods have been developed to obtain hierarchical structures. Among these methods, casting technique shows special attraction due to its simple process of preparation. For example, uniform vesicle in microscale could be transferred onto the substrate to obtain a honeycomb structure by this method [14]. We also obtained stripe aggregated structures by using an amphiphilic block molecule with oligo(phenylene vinylene) as rod and poly(ethylene oxide) as coil on solid substrate through controlled solvent evaporation [15,16]. Among those driving forces for fabricating hierarchical self-assemblies, hydrogen bonding is proved to be convenient and effective in the preparation of organized systems and functional

* Corresponding author. Fax: +86 431 5193421.
E-mail address: wulx@jlu.edu.cn (L. Wu).

0032-3861/$ - see front matter © 2007 Elsevier Ltd. All rights reserved.
doi:10.1016/j.polymer.2007.04.041

supramolecular structures, especially for the complex building blocks [17–20]. In most cases, multiple hydrogen bonds are needed to strengthen the connection force between different components [21,22]. However, self-assembling structures constructed through single hydrogen bond in solution [23–25], liquid crystal [18] and sol–gel system [26] have also been reported.

Considering the environment sensitivity of component structure and the tunable property of hydrogen bonded building blocks, we try to apply the components with large diversity in molecular length, volume ratio, rigidity and flexibility as well as hydrophobic and hydrophilic properties to build hydrogen bonding complex. By selecting suitable hydrogen bond donor–acceptor pair, a rigid dendritic block (L1) and a flexible poly(ethylene oxide) with stilbazole terminal group part ($PyEO_{12}$) are employed to prepare complex 1. We expect to obtain hierarchical self-assemblies based on the hydrogen bonded diblock complex and control the morphologies of its aggregates in solution through careful tuning of solvent polarity and concentration. Complicated hierarchical structures of this diblock complex are constructed through transferring the aggregates onto solid substrate by simply casting. Especially, these hierarchical structures are proved to be at a much higher organized level through order arrangement of complicated aggregates on solid substrate rather than at gas–liquid and/or liquid–solid interfaces [27,28].

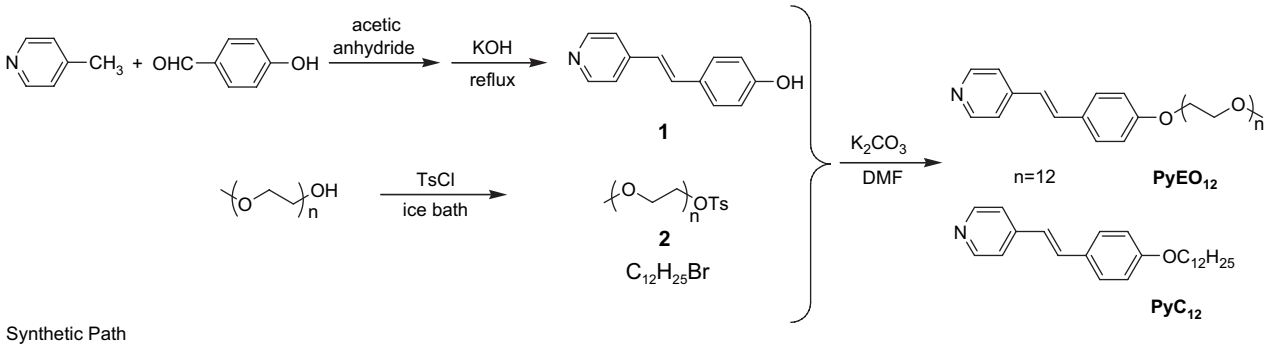

Synthetic Path

2. Experimental section

2.1. Synthesis

2.1.1. trans-4-[2-(4′-Phenol)vinyl]pyridine (1)

A mixture of 4-hydroxyl benzaldehyde (12.2 g, 100 mmol) and 4-methyl pyridine (10.2 g, 110 mmol) was dissolved in anhydride acetate and stirred at 125 °C for 8 h. After cooling to room temperature the precipitate was collected by suction under reduced pressure and recrystallized from ethanol to give the product ester of acetate. To 150 mL of mixed solution of ethanol and water (volume ratio 1:1) were added the ester solid (10.0 g, 28 mmol) and potassium hydroxide (4.0 g, 71 mmol), and then the solution was refluxed for 6 h. The resulting reaction mixture was neutralized by the addition of diluted hydrochloride acid dropwise. The precipitate was collected by filtration, drying to give (1) (11.2 g, 57 mmol) in 57% yield as a pale yellow solid. ^{1}H NMR (500 MHz, $CDCl_3$, TMS): 6.79–6.81 ppm (d, $J = 8$ Hz, 1H), 7.02 ppm (d, $J = 16$ Hz, 1H), 7.45 ppm (d, $J = 16$ Hz, 1H), 7.49 ppm (t, $J = 4$ Hz, 4H), 8.50 ppm (d, $J = 5$ Hz, 2H), 9.74 ppm (s, 1H).

2.1.2. p-Toluenesulfonyl poly(ethylene oxide) monomethyl ether (2)

To the mixture of poly(ethylene oxide) monomethyl ether (EO, 550, $M_w/M_n = 1.03$) (11 g, 20 mmol), the commercial product from Fluka, and 24% sodium hydroxide aqueous solution (5.5 mL) in an ice bath was added dropwise THF (15 mL) solution of *p*-toluenesulfonyl chloride (4.2 g, 22 mmol) with continuous stirring at 0 °C. The resulting mixture was further stirred at 0 °C for 6 h and then poured into ice water. The aqueous solution was extracted with three portions of chloroform (20 mL). The combined organic extracts were dried over anhydrous $MgSO_4$, filtered and concentrated under reduced pressure. The residue was purified by column chromatography on silica gel with chloroform as an eluent followed by 10:1 of chloroform/methanol to give 3.0 g (1.85 mmol) of product (2) in 93% yield as a colorless oil. ^{1}H NMR (500 MHz, $CDCl_3$, TMS): 3.37 ppm (s, 3H), 3.58–3.73 ppm (m, 46H), 4.16 ppm (t, $J = 5$ Hz, 2H), 7.35 ppm (d, $J = 8$ Hz, 2H), 7.80 ppm (d, $J = 8$ Hz, 2H).

2.1.3. trans-4-{2-[4-Oligo(oxyethylene)oxyphenyl]vinyl}-pyridine ($PyEO_{12}$)

A mixture of (1) (2.0 g, 10 mmol), (2) (3.0 g, 5 mmol), and K_2CO_3 (2.0 g, 15 mmol) in DMF (50 mL) was stirred at 100 °C for 24 h under N_2 atmosphere. DMF was then removed under reduced pressure and the residue was redissolved in chloroform. The organic phase was washed with water and brine, dried over anhydrous $MgSO_4$, and filtered. The excess solvent was evaporated off and the crude product was purified by column chromatography on silica gel with 15:1 of ethyl ether/methanol as an eluent followed by 10:1 of chloroform/methanol to give $PyEO_{12}$ (2.75 g, 4.2 mmol) in 85% yield as a pale yellow oil at room temperature. ^{1}H NMR (500 MHz, $CDCl_3$, TMS): 3.37 ppm (s, 3H), 3.58–3.73 ppm (m, 46H), 4.16 ppm (t, $J = 5$ Hz, 2H), 6.88 ppm (d, $J = 16$ Hz, 1H),

6.92 ppm (d, $J = 8$ Hz, 2H), 7.26 ppm (d, $J = 16$ Hz, 1H), 7.35 ppm (d, $J = 4$ Hz, 2H), 7.47 ppm (d, $J = 8$ Hz, 2H), 8.54 ppm (d, $J = 5$ Hz, 2H). MALDI-TOF MS: *m/z*: 651.2 [M^+], 695.7 [M^+], 739.1 [M^+], 783.1 [M^+], 831.8 [M^+], 871.2 [M^+]. $M_w/M_n = 1.01$.

2.1.4. trans-4-[2-(4-Dodecylphenol)vinyl]pyridine (PyC_{12})

trans-4-[2-(4-Dodecylphenol)vinyl]pyridine was previously synthesized according to the literature [29].

2.1.5. 3,4,5-Tris{3,4,5-tris[n-(cetane-1-yloxy)benzyloxy]-benzyloxy}benzoic acid (L1)

L1 was synthesized according to a reported method without modification [30]. ^{1}H NMR (500 MHz, $CDCl_3$, TMS): 0.87 ppm (t, 27H), 1.25 ppm (m, 264H), 1.42 ppm (m, 18H), 1.71 ppm (m, 18H), 3.88 ppm (m, 18H), 5.04 ppm (d, $J = 5$ Hz, 6H), 6.59 ppm (s, 2H), 6.63 ppm (s, 4H), 7.43 ppm (s, 2H).

2.2. Sample preparation

The complex (1) solution was prepared by mixing $PyEO_{12}$ (average molecular weight) and L1 with 1:1 molar ratio in the mixed solvent of toluene and DMSO and underwent a 20-min sonication at room temperature. After standing overnight, the solution was cast dropwise onto a silicon wafer until the solvent was naturally evaporated to dryness in air. Samples for SEM were coated with a very thin film of gold before measurement.

The samples for TEM were prepared by immersing a carbon-coated copper grid in the solution, and the excess solvent was sucked with filter paper to dryness. The samples for AFM were prepared by casting mixed solution on the silicon wafer and quickly removing the excess solution with filter paper. The samples for FT-IR spectra were prepared by casting the concentrated solution onto KBr tablets.

2.3. Measurements

FT-IR spectra were performed on a Bruker IFS66V FT-IR spectrometer equipped with a DGTS detector (256 scans). The spectra were recorded with a resolution 4 cm^{-1}. ^{1}H NMR spectra (TMS) were carried out on a Bruker UltraShield™ 500 MHz spectrometer. The small-angle X-ray diffraction (SAXRD) of thick casting film on silicon wafer was characterized on a Rigaku X-ray diffractometer (D/max rA, using Cu Kα radiation with the wavelength of 1.542 Å). MALDI-TOF spectra were recorded on a Kratos-Shimadzu AXIMA-CFR mass spectrometer. The optical photographs were obtained on a FUJIFILM A202 camera. Scanning electron microscopy (SEM) images were obtained with Shimadzu SSX-550 Superscan and FEI XL 30 using ESEM and operating at an accelerating voltage of 25 kV. Atomic force microscopic (AFM) images were obtained with a commercial instrument (Digital Instrument, Nanoscope III, and Dimension 3000™), operating in tapping mode at room temperature in air. Transmission electron microscopic (TEM) images were obtained on a HITACHI H 8100 TEM with an accelerating voltage of 200 kV without staining. Contact angle analysis (CA) was performed on a DSA 10 MK2 (a drip is 8 μL). The dynamic light scattering (DLS) was carried out on a Wyatt DAWN EOS Enhanced Optical System at 20 °C.

3. Results and discussion

3.1. Hydrogen bonding of the complex

Scheme 1 shows the structure of complex 1, which is composed of a hydrophobic dendritic donor, L1, and a hydrophilic flexible stilbazole-containing EO acceptor, $PyEO_{12}$. The casting film and the solution (mixture of toluene and dimethylsulfoxide) of complex 1 were characterized by FT-IR spectral (Fig. 1) and dynamic light scattering (DLS) measurements (Fig. 2), respectively. The disappearance of O–H stretching band at 3300 cm^{-1} and the appearance of the absorption band at 1937 cm^{-1} provide the evidence for the formation of hydrogen bond between $PyEO_{12}$ and L1. The C=O stretching vibration of L1 at 1683 cm^{-1} cleaves into two bands and shifts to 1700 and 1730 cm^{-1}, respectively, also confirming the existence of intermolecular hydrogen bond in the casting film of complex 1 [31,32]. The hydrodynamic radius R_h of complex 1 aggregates at 1×10^{-4} M was measured to be about 120 nm (Fig. 2a), much larger than that of single-component L1

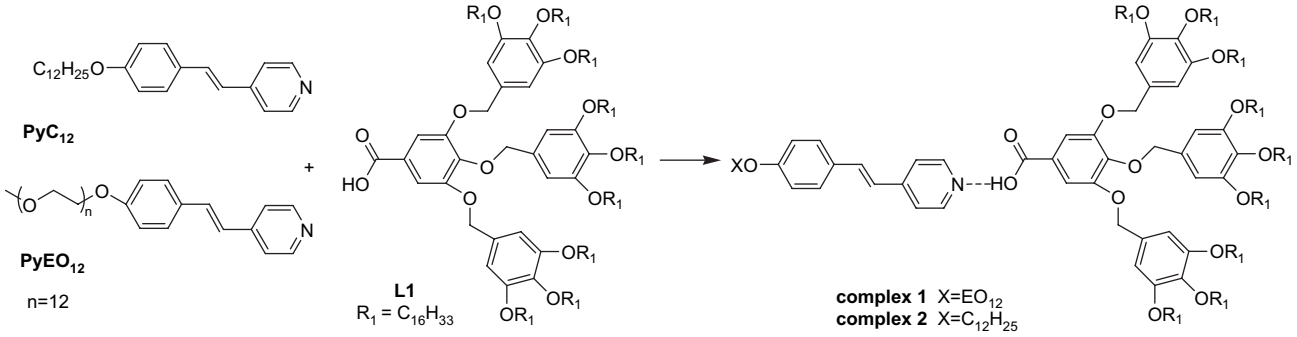

Scheme 1. Schematic chemical structures of complex 1 and complex 2, which are composed of grafted L1 with $PyEO_{12}$ and PyC_{12} through hydrogen bonding, respectively.

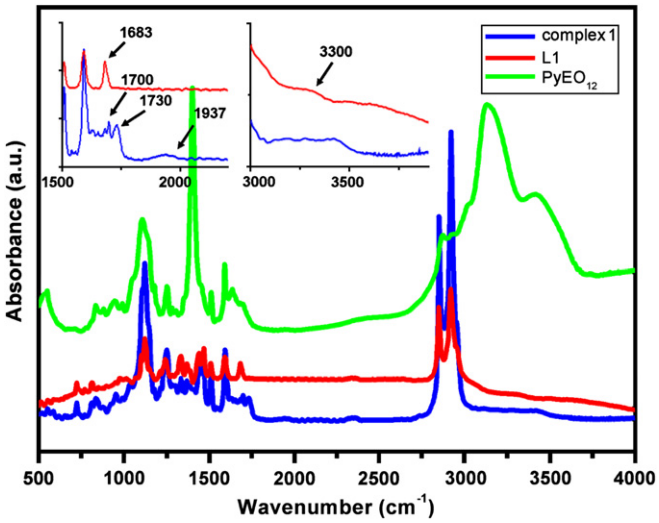

Fig. 1. FT-IR spectra of complex 1 and its separated components in solid state.

aggregates, which is found to be about 52 nm (Fig. 2b) in the mixed solution of 20:1 toluene/DMSO (v/v). The large size difference of aggregation between L1 and complex 1 implies the stable existence of intermolecular hydrogen bonding in solution, which leads to a large increase of R_h of complex 1. We believe that the stable hydrogen bonding is possibly assisted by the contribution of strong amphiphilic interaction from the two-component aggregation in the mixed solution although the percentage of hydrogen bonding between L1 and $PyEO_{12}$ cannot be estimated exactly.

3.2. Transformation of aggregation morphologies

By simply varying the concentration of complex 1 such as solvent polarity based on the volume ratio of toluene and DMSO and the casting volume of solution, diverse self-assemblies including sphere, fiber, entangled structures, and the transformation among them can be obtained and characterized by SEM, as shown in Fig. 3. The observed spherical structures are hollow and possess a diameter of 200–300 nm, and the fibers are found to be composed of elementary cylindrical micelles based on the surface dents and grooves as shown in the insets of Fig. 3a and b. Interestingly, more complicated hierarchical architectures, wreath-like and hollow entanglement structures are observed (Fig. 3c and d), which can be inferred to be composed of more tangled fibers with increasing sample concentration. Evidently, the wreath-like structure is derived from the incomplete spinning of twisted fibers and the hollow entanglement structures are attributed to almost complete spinning of abundant twisty fibers on the wreaths.

Based on the observation of various self-assembled structures of complex 1 it is certain that there are transformations among the aggregation morphologies. The primarily formed spheres can gradually translate into cylindrical micelles with increasing concentration, which is similar to the case occurred in the general surfactant aggregation system [33,34]. Keeping the mixing ratio (20:1 in v/v) of the mixed solvent and the identical preparing procedure, as shown in Fig. 4, spherical aggregates obtained through rapid evaporation are observed by TEM under lower concentration, 1.5×10^{-4} M and 2.5×10^{-4} M (Fig. 4a and b), respectively. When increasing the concentration up to 5×10^{-4} M, however, rough fibrous aggregates with branches and knots start to emerge, which are obviously derived from the fusion of the original spherical aggregates (Fig. 4c). When the concentration rises up to 1×10^{-3} M, the spherical aggregates disappear completely and fibrous aggregates are observed instead (Fig. 4d), further indicating the concentration-dependent transformation of aggregation morphologies. For the gelation transformation of amphiphilic coil–rod–coil molecules, it is confirmed to rely on the addition of another rod–coil–rod component acting as the linking agent of originally formed cylindrical micelles [35]. Remarkably, in contrast to that, complex 1 itself can change slowly from fluid phase (Fig. 5a) into a transparent organogel in the concentrated solution (about 3 mg/mL) after a few days' standing at room temperature (Fig. 5b). The gelation of complex 1 indicates that canned bundles of primary cylindrical micelles can spontaneously be prolonged and finally entangle into cross-linked three-dimensional network structure [36]. Therefore, the transformation process can be well controlled by varying concentration and we believe that it is a thermodynamically stabilized process at high concentrated solution, which could be attributed to the space requirement of crowded alkyl chains of dendron block because the fibrous

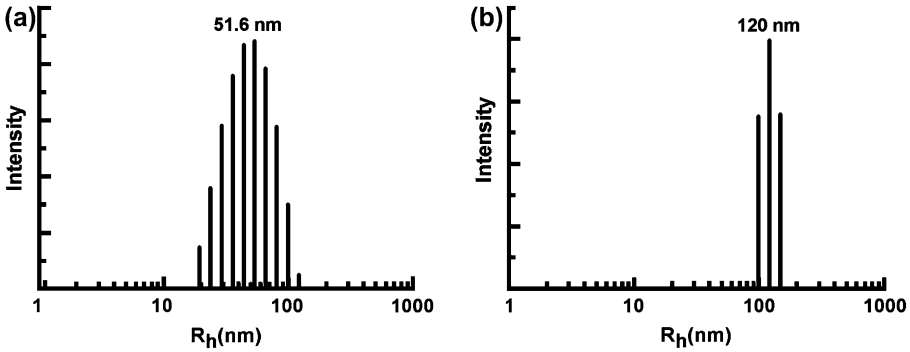

Fig. 2. DLS graphs of 1×10^{-4} M of (a) separated component L1 and (b) complex 1 in dilute mixed solution of toluene/DMSO of 20:1 (v/v), respectively. R_h is 51.6 nm for component L1 and 120 nm for complex 1, respectively.

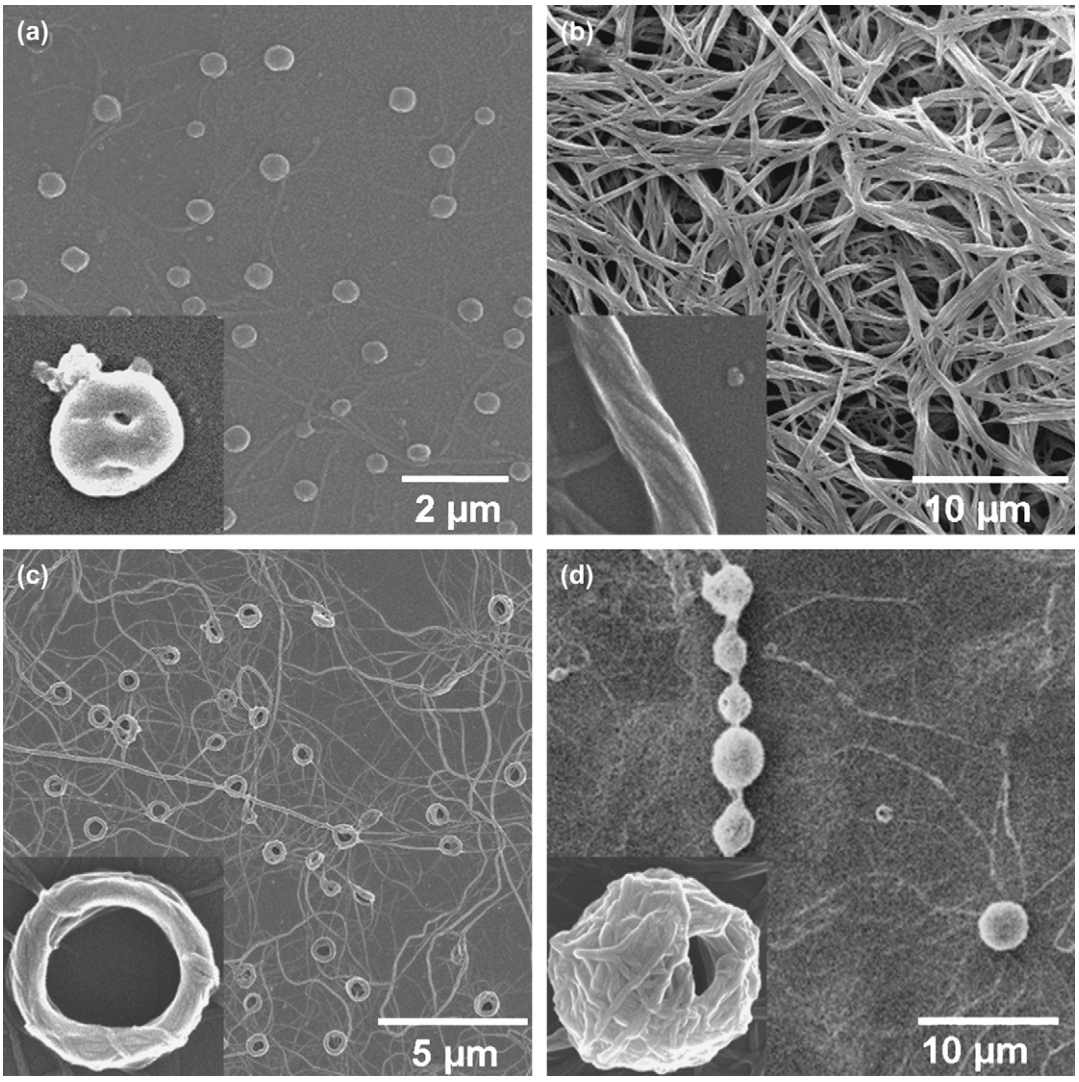

Fig. 3. SEM images of various self-assembling structures by casting complex 1 solution on silicon substrate: (a) spherical vesicular structure by casting small amount of 1×10^{-4} M sample solution, (b) fiber structure by casting small amount of 1×10^{-3} M sample solution, (c) hierarchical wreath-like structure by casting suitable 1.5×10^{-4} M sample solution with toluene and DMSO volume ratio of 10:1, respectively, and (d) hierarchical entanglement structure by casting excess 3×10^{-4} M sample solution with toluene and DMSO volume ratio of 10:1.

structure provides a larger curvature and more space than that of spherical vesicle.

3.3. Aggregation structure of the complex

The spherical aggregates in dilute solution were examined to possess a vesicular structure by AFM measurement. By casting the mixed solution of complex 1 (1.5×10^{-4} M) onto a silicon wafer and quickly removing excess solvent with a piece of filter paper, spherical aggregates are observed. The measured statistic height and diameter of spherical aggregates are about 22.8 nm and 286 nm, respectively. Considering shape-induced and tip radius-induced errors (7.6–15.2 nm and 15.9 nm, respectively), the exact diameter of spherical aggregates should be 254.9–262.5 nm. This value is little bit larger than the one from DLS, 240 nm. This is reasonable and possible because there will be a scale increasing of aggregates during spherical aggregates being compressed into a dried pie aggregates. But in any case, the present comparison is rough as there are a lot of factors to affect the size when transferring the aggregates from solution to the solid substrate through the evaporation of solvent. For the height of spherical aggregates, in contrast to its diameter, is very short and just corresponding to the double bilayer thickness of complex 1, which is simulated from the result of SAXD. Generally, for soft vesicles, the AFM height image (Fig. 6) and TEM micrograph are not often presented typically like those of undeformed ones. For example, the identification of the staved vesicles formed by dendritic–dendritic copolymers was done through the phase analysis of AFM image because the high periphery and lower center morphology was seen from AFM rather than TEM image due to the deformation of the aggregated objects during the deposition and measurement [37]. In view of the dented aggregates in phase image together

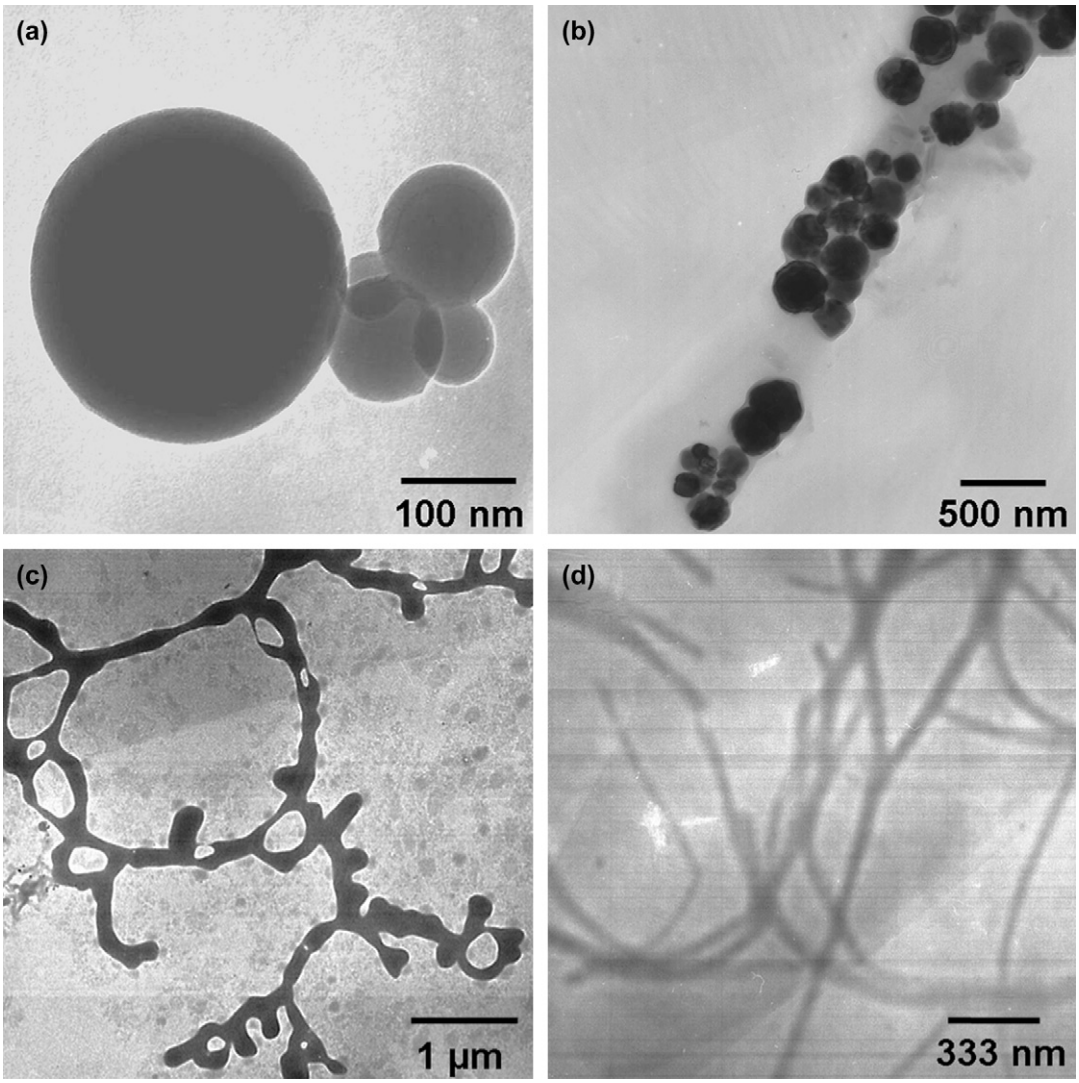

Fig. 4. TEM images of complex 1 aggregates obtained by casting its mixed solution of toluene and DMSO (20:1 in v/v) at the concentration of (a) 1.5×10^{-4} M, (b) 2.5×10^{-4} M, (c) 5×10^{-4} M, and (d) 1×10^{-3} M, respectively.

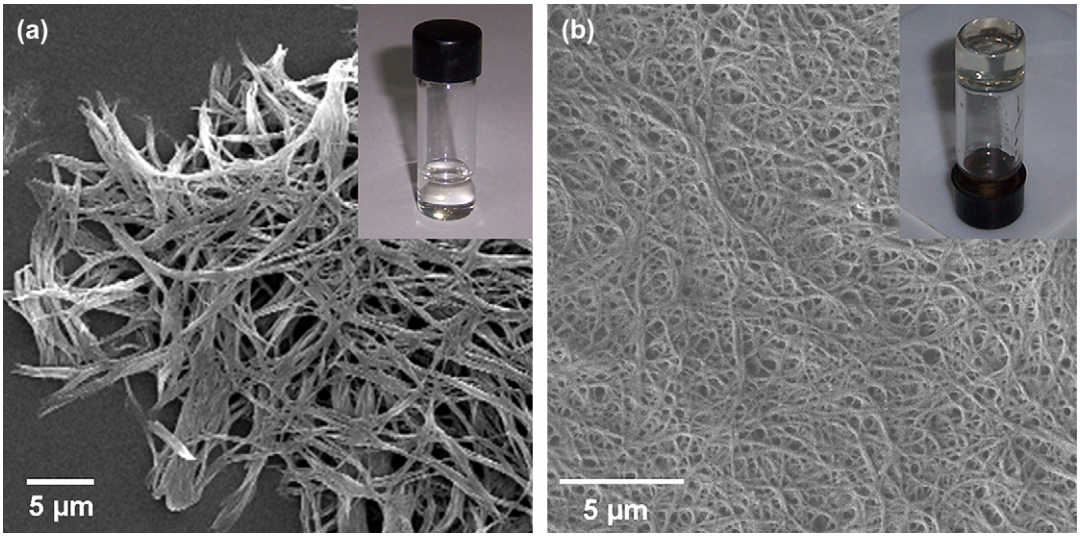

Fig. 5. SEM (a) images and inserted photographs of fresh solution and (b) transparent organogel of complex 1 under the concentration of 1×10^{-3} M (3 mg/mL) in the mixed solvent with toluene and DMSO ratio of 20:1 (v/v), respectively.

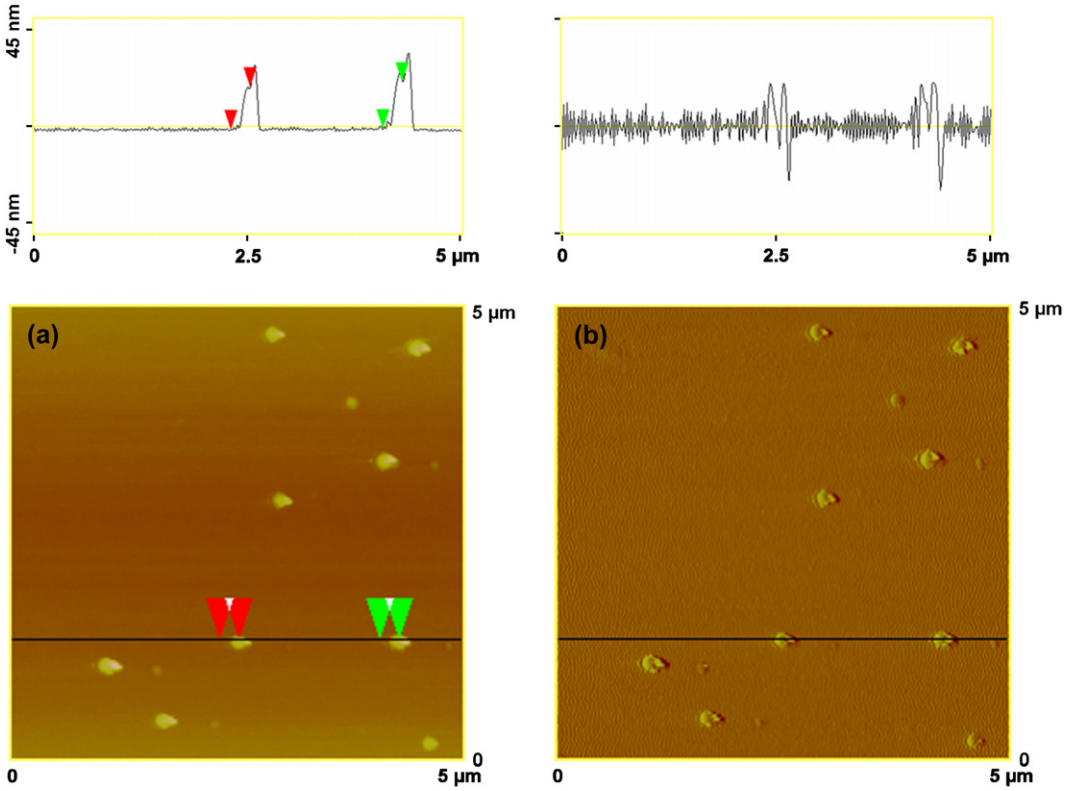

Fig. 6. AFM (a) height and (b) phase images of deformed complex 1. The spherical aggregates are obtained by casting its 1.5×10^{-4} M mixed solution with toluene/DMSO of 10:1 and removing the excess solvent rapidly.

with the measured height in our case, which is similar to that reported in the literature, we infer that the spherical aggregates (Fig. 3a) are hollow vesicles. The speculation also can be supported by SEM and TEM measurements independently. When the spherical aggregates on silicon wafer have been annealed in vacuum for 6 h, a mass of cracked spheres is observed by SEM (Fig. 7a). Especially, the cracked spherical aggregates with weak contrast were observed from TEM image (Fig. 7b) by increasing solvent polarity of lower concentration solution. All these characteristics indicate that the hollow vesicle of complex 1 mainly exists in diluted solution.

By casting the concentrated solution with low polarity on solid substrate repeatedly the fabricated self-assembly structure can be controlled to consist of fibers mainly, as confirmed

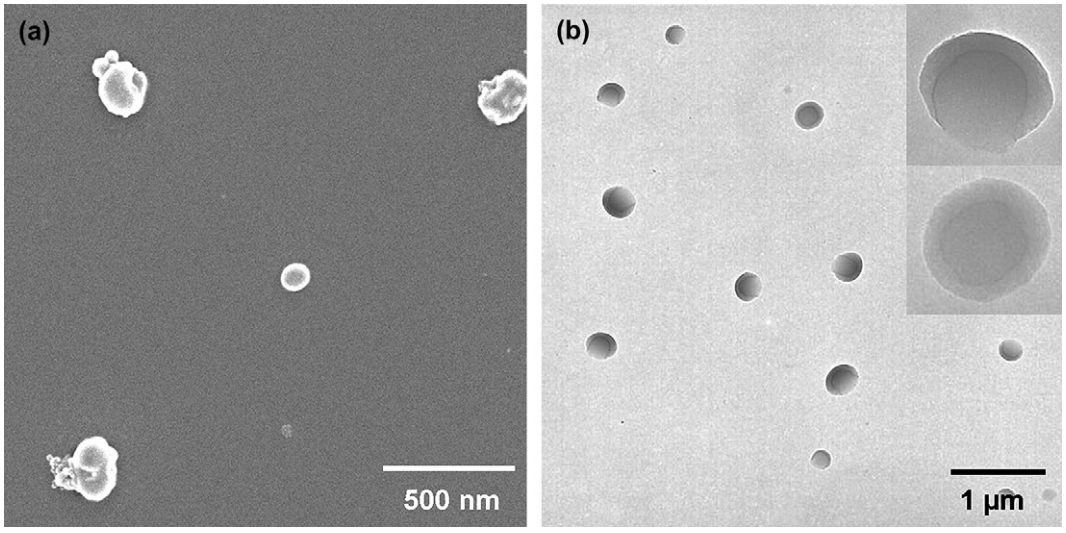

Fig. 7. SEM and TEM images of complex 1, in which (a) deformed vesicles were obtained by casting its 1.5×10^{-4} M mixed solution with toluene and DMSO of 5:1, and standing in vacuum for 6 h, (b) the cracked vesicles were obtained by increasing polarity of mixed solution to the volume ratio of 1:1.

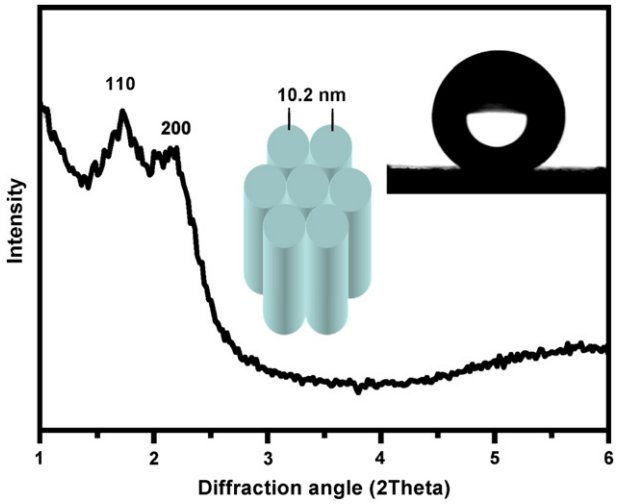

Fig. 8. SAXRD pattern of thick film of complex 1 fibers and contact angle photograph of the film (inset).

by SEM (Fig. 3b). From the SAXRD measurement (Fig. 8), the q ratio according with $\sqrt{3}:2$ suggests that the fibers are constructed by elementary cylindrical micelles with hexagonal columnar arrangement. So, the diameter of elementary cylindrical micelle is estimated to be 10.2 nm ($a = d_{100} \times 2/\sqrt{3}$). The estimated diameter is smaller than the double length of fully extended complex 1 but it seems rational if we consider the folding and filling of flexible EO block in the cylindrical micelle. The fiber structure can also be further demonstrated by AFM measurement independently (see Supplementary data). By casting concentrated sample solution (1.5×10^{-3} M, 20:1 v/v) on silicon wafer and then quickly removing the extra solvent, a single fiber can be observed. From the magnified phase images, we propose that the fiber is composed of elementary cylindrical micelles with a width of 10–12 nm, which is just corresponding to the diameter of elementary cylindrical micelle deduced from SAXRD data. Meanwhile, the thick casting film of the fibers shows a water contact angle (CA) of $153 \pm 1°$ (Fig. 8, inset). Besides the influence of the special surface structure on the contact angle, the superhydrophobicity suggests a hydrophobic surface of the fiber as well. Therefore, we suppose that the EO block locates at interior part as a core and the dendritic block locates at exterior part as a shell in the cylindrical micelle [30,38]. Considering the hydrophobic property of alkyl chains and volume ratio of dendritic and linear blocks, such a stacking structure should be favorable in space.

3.4. Hierarchical self-assembling of the complex

By controlling evaporation condition, the fibers sequentially self-assemble into wreath-like and finally into hollow entanglement structures at the last stage of natural evaporation because we distinctly see the spinning of the fibers on these wreaths and hollow entanglement structures, as shown in Fig. 3c and d. Linear–dendritic–rod triblock copolymer in tetrahydrofuran/water mixed solution can self-assemble into ring-like aggregate, which was explained resulting from the fusion of cylindrical micelles, which is assisted by the addition and connection of another semirod–coil–semirod molecules [39]. But in the present case, besides the weak hydrophobic and concentration-driven forces there is no additional interaction in the dendritic–coil block structure for the fusion of cylindrical micelles, even taking account of other similar systems such as dendritic–linear, linear–linear and dendritic–dendritic diblock copolymers other than rod–coil–rod and coil–rod–coil triblock copolymers [40]. Therefore, the wreath-like aggregates should be derived from the simple intertwist of micelle bundles. To the best of our knowledge, the novel hierarchical self-assembling wreath-like aggregates are firstly obtained through bottom-up growth of wedge-like complex on the solid substrate. Considering that the employed solvent is a mixture of two solvents with different polarity and boiling point, and the velocity of volatilization of DMSO is slower than that of toluene due to its higher boiling point, the solvent polarity will increase along with the evaporation, especially at the last stage. So we believe that both the polarity of solvent and the amphiphilic property of the complex are involved in the formation of the hierarchical structures.

To identify the morphology dependence of the fibrous assemblies on the solvent polarity, the organized behavior of complex 1 is further examined by adjusting the mixing ratio of toluene and DMSO. When the sample concentration is kept at 1.5×10^{-3} M, the linear fibrous assemblies are found to exist as main aggregates and tend to be twisty accompanied by increasing the content of DMSO (Fig. 9). Due to the miscibility of $PyEO_{12}$ block of complex 1 in DMSO, the increase of the solvent polarity facilitates the amount of DMSO contained in $PyEO_{12}$, thus decreases the interaction between $PyEO_{12}$ blocks and the packing density (or crystalline tendency), which consequently leads to more flexible cylindrical micelles. To confirm this speculation, complex 2, an analogue of complex 1, in which hydrophilic $PyEO_{12}$ chain is replaced by hydrophobic alkyl chain, is chosen as a contrast against the polarity-induced morphological change of complex 1. Only straight fibers rather than wreath-like or entanglement structures are observed under the same condition. The reason for complex 2 forming only straight fibrous structure can be attributed to its more hydrophobic rigid core than that of complex 1 fiber under the same condition of polarity. The result can be further supported by the fact that when $PyEO_{12}$ block is replaced by much more rigid groups, 1,2-bis(4-pyridyl)ethylene and 1,4-bis(4-vinylpyridyl)phenylene, their complexes with L1 form neither the wreath-like nor the entanglement structure besides straight fibers at the same polarity condition.

The polar DMSO in the mixed solution plays important roles not only in the adjustment to the polarity of solvent but also in the formation of wreath-like and hollow entanglement hierarchical structures. By putting a drop of pure mixed solvent with 10:1 (v/v) of toluene and DMSO onto a glass slide, the dispersion and evaporation processes are carefully examined by optical microscopy. With the evaporation of solvent, DMSO starts to separate from toluene and forms isolated small droplets on solid surface at the end of toluene

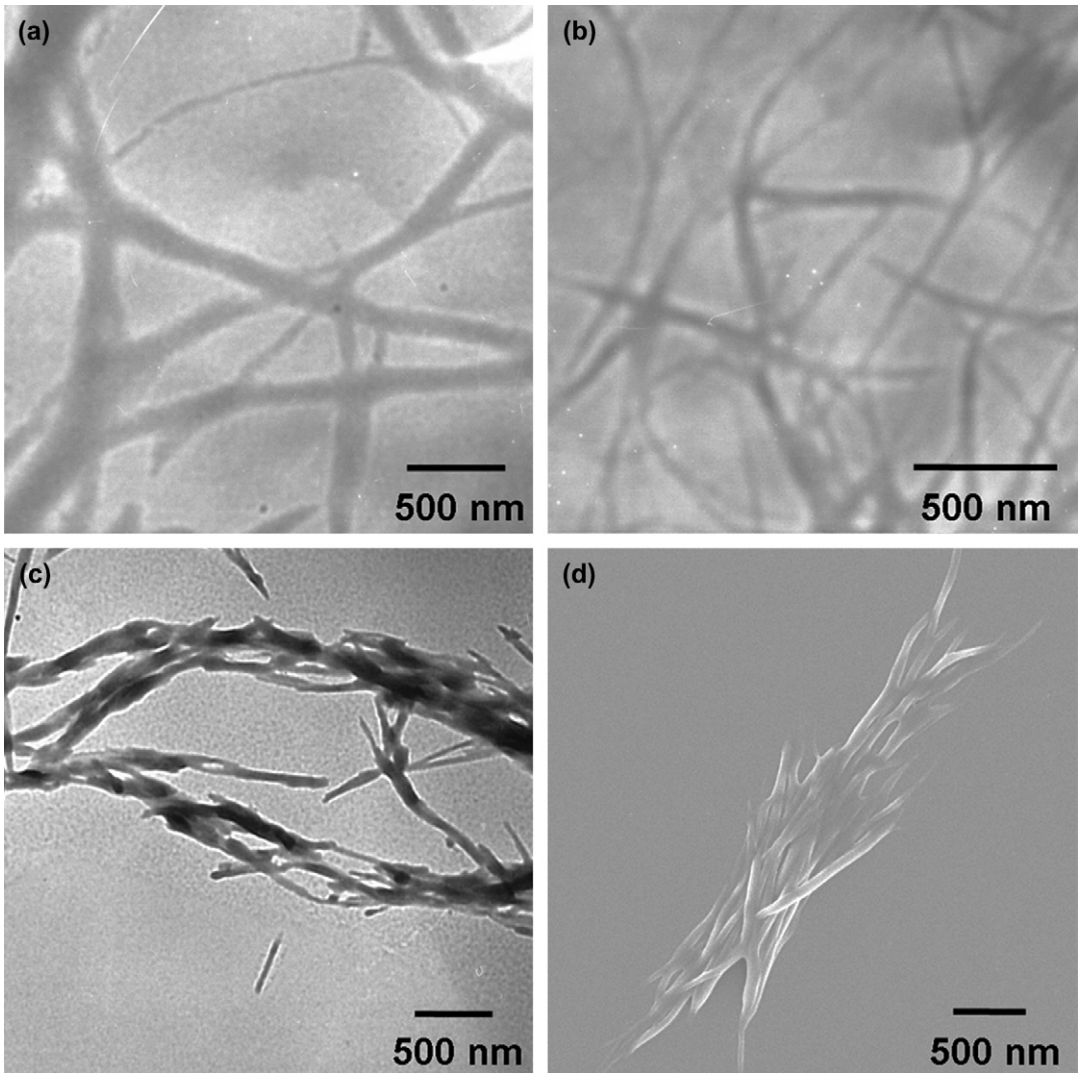

Fig. 9. TEM images of complex 1 aggregates in concentrated mixture solution (1.5×10^{-3} M) versus the solvent polarity with the volume ratio of toluene and DMSO at (a) 20:1, (b) 10:1, (c) 5:1, respectively, and (d) SEM image of the sample (c).

evaporating off completely. Under the case that the pure mixed solvent is replaced by complex 1 sample solution, systematic changes in endgame of the evaporation are observed, as exhibited in Fig. 10. The fibrous aggregates are soluble in the mixed solvent on the substrate initially, then gradually become indiscerptible and shrink away to the interface between toluene and DMSO droplets with the evaporation of toluene (Fig. 10b and c). When the whole toluene is evaporated to dryness, the fibers attach on the surface of DMSO droplets because of the high surface tension, which leads to a hierarchical fiber architecture possessing hydrophobic surface (Fig. 10d and e). After DMSO droplets also evaporate off completely, the fibers absorbed on the surface of DMSO spots leave over on the substrate and form wreath-like structure (Fig. 10f). In contrast to this result, by using pure toluene instead, only linear structure of complex 1 is gathered. When increasing the casting concentration to increase the amount of fibers in the complex solution the wreath-like structure develops to hollow entanglement structure because in this case DMSO droplets can be fully covered by excess fibers. Independent wreath-like or entanglement structures could be obtained through controlling casting concentration, polarity and dripping volume. For example, by fixing the solution polarity under the ratio of toluene and DMSO at 8:1–20:1 (v/v), we can selectively obtain wreath-like or hollow entanglement architectures in a large area mainly.

Interestingly, when casting 1.5×10^{-4} M of sample solution with mixing ratio of 20:1 on silicon wafer, all five self-assembled structures can be clearly observed from the outside edge to the center of the spreading field in one step (Fig. 11a). Vesicles appear in the beginning of evaporation and locate at the outside edge of the casting area (Fig. 11b); fibers and pearl-necklace structures mainly appear in the middle region at the interim stage of evaporation (Fig. 11c and d); and wreath-like and hollow entanglement structures locate at the central part at the endgame of evaporation (Fig. 11e and f). The evolution of the aggregation structure with natural evaporation also supports the conclusion that there is

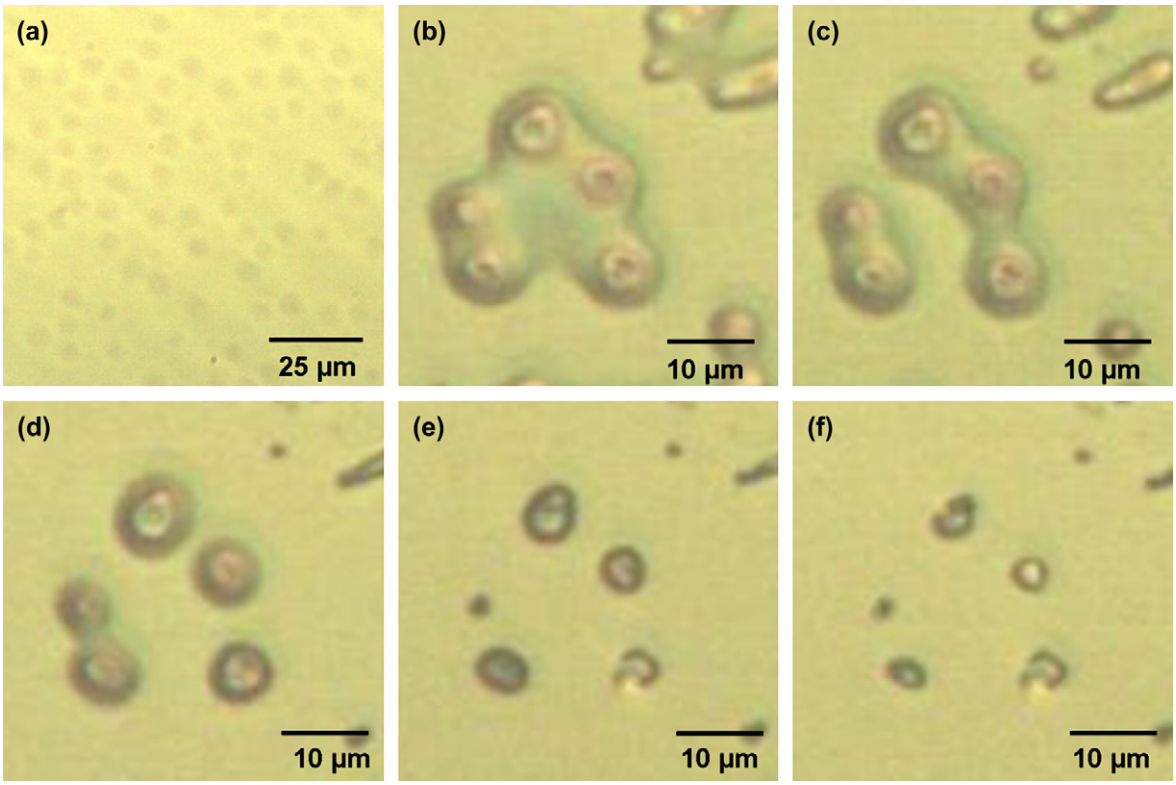

Fig. 10. Optical microscopic photos of (a) pure mixed solvent with toluene and DMSO volume ratio of 10:1, (b–e) various stages of natural evaporation until to (f) dryness on the silicon substrate by casting complex 1 solution (1.5×10^{-4} M) with toluene and DMSO volume ratio of 10:1.

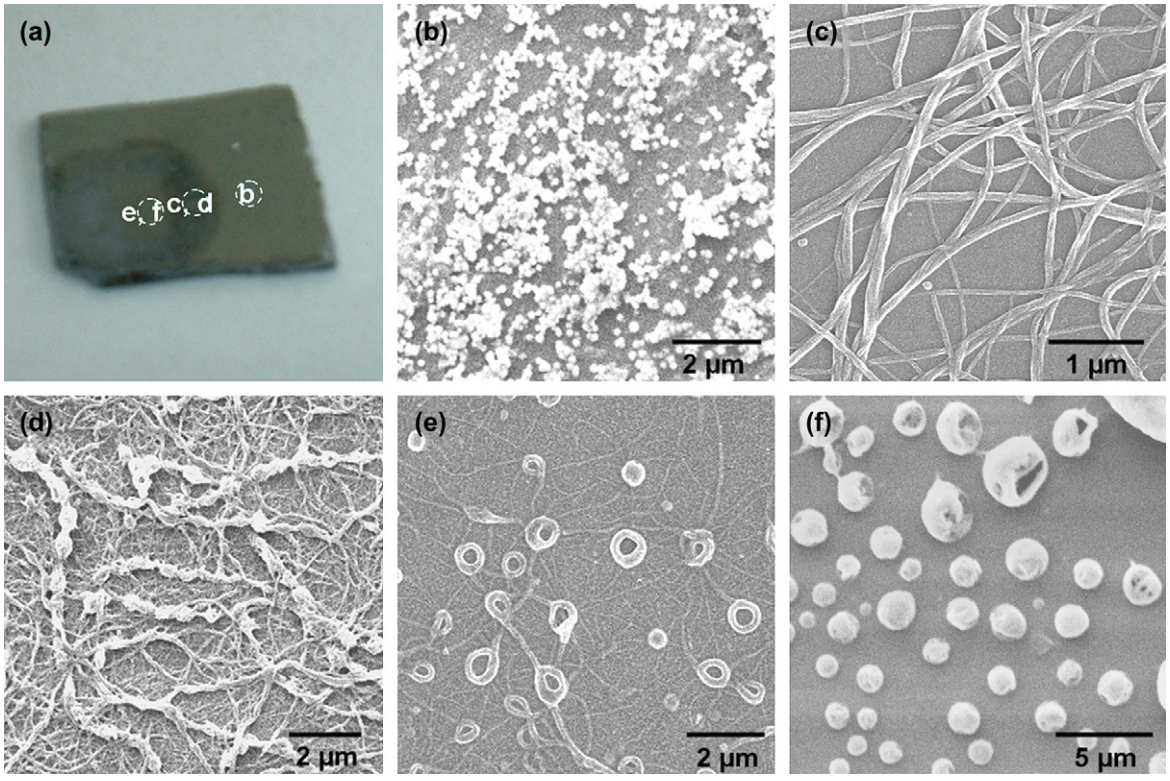

Fig. 11. Optical photograph and SEM images of the superstructures at different regions of the casting film of 1.5×10^{-4} M complex 1 mixed solution with 20:1 of toluene/DMSO on a silicon substrate. (a) Optical photograph of outside view of the silicon wafer, (b) spherical structure at the edge of casting field, (c) and (d) fibrous and pearl-necklace structures in the middle area of casting field, (e) and (f) hierarchical wreath-like and entanglement structures at the site near the central area of the casting field.

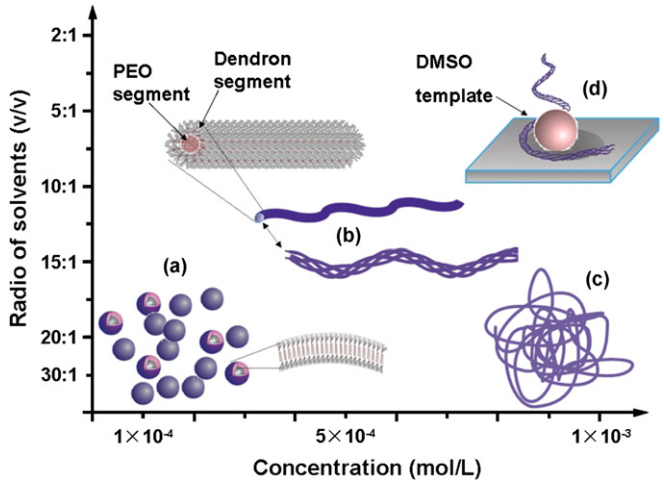

Fig. 12. Schematic representation of various self-assembled structures of complex 1 versus the forming condition.

a transformation of self-assemblies from vesicle to cylindrical micelle with increasing concentration and polarity, because both of them are gradually increasing in the process of evaporation.

From the above data and analysis, we propose a possible model for understanding various self-assembled structures formed by the hydrogen bonded complex 1 in solution and on the solid substrate (Fig. 12). Vesicles mainly exist in the solution at lower concentration (Fig. 12a), where $PyEO_{12}$ block interlayered between double dendritic block layers can hold DMSO molecules, leading to a curved lamellar structure. The transformation from vesicle to cylindrical micelle occurs while increasing concentration. Here, the cylindrical micelle of complex 1 is more stable because the crowded dendron blocks need more space for their stacking capacity at concentrated solution, just as the self-assembling of low-weight amphiphilic molecules in the similar condition (Fig. 12b) [34,35]. The fibers grow and further branch and entangle into three-dimensional network structure forming transparent organogel by standing. Transferring the mixed solution of complex 1 onto the solid substrate by casting method, dispersive DMSO droplets leave on the substrate after the evaporation of toluene to dryness and flexible fibers fasten and spin to assemble into hierarchical wreath-like and entanglement structures with the DMSO leftover as template (Fig. 12d). The wreath-like and entanglement structures are easily dominated by the casting volume and solution concentration.

4. Conclusions

In conclusion, a single hydrogen bond complex composed of dendritic and linear block molecules as an amphiphilic building block can be applied for the construction of supramolecular self-assemblies. This kind of complex not only has specific geometric shape, amphiphilic property and enough flexibility, but also forms various self-assemblies such as vesicles and cylindrical micelles in two-component solution by adjusting preparation condition. Interestingly, these novel hierarchical self-assemblies based on primary cylindrical micelles obtained by present procedure are different from previously reported superhelical structures [41]. The main factors for the formation of the complicated self-assembled structures are the polarity separation of solvent components and the template effect of DMSO in the casting film due to its difference of evaporation velocity from toluene. The gelatification and superhydrophobicity of the self-assembled structures are significant for exploitation of new functional materials. Importantly, the present results may provide a convenient route for understanding the nature of self-assemblies of complicated systems and structures.

Acknowledgments

We acknowledge the financial support from National Basic Research Program (2007CB808003), National Natural Science Foundation of China (20574030), PCSIRT of Ministry of Education of China (IRT0422), and Open Project of State Key Laboratory of Polymer Physics and Chemistry of CAS. We thank Professor F. Schue from University of Montpelier for the helpful discussion on the occasion of visiting us, supported by 111 project (B06009).

Appendix. Supplementary data

Supplementary data associated with this article can be found in the online version, at doi:10.1016/j.polymer.2007.04.041.

References

[1] Lehn J-M. Supramolecular chemistry. New York: VCH Press; 1995.
[2] Service RF. Science 2005;309:95.
[3] Alper J. Science 2002;295:2396–7.
[4] Shimizu T, Masuda M, Minamikawa H. Chem Rev 2005;105:1401–43.
[5] Uzun O, Sanyal A, Nakade H, Thibault RJ, Rotello VM. J Am Chem Soc 2004;126:14773–7.
[6] Hu Z, Jonas AM, Varshney SK, Gohy J-F. J Am Chem Soc 2005;127:6526–7.
[7] Cornelissen JJLM, Fischer M, Sommerdijk NAJM, Nolte RJM. Science 1998;280:1427–30.
[8] Engelkamp H, Middelbeek S, Nolte RJM. Science 1999;284:785–8.
[9] Klok H-A, Jolliffe KA, Schauer CL, Prins LJ, Spatz JP, Moeller M, et al. J Am Chem Soc 1999;121:7154–5.
[10] Ryu JH, Kim HJ, Huang ZG, Lee E, Lee M. Angew Chem Int Ed 2006;45:5304–7.
[11] Choi IS, Bowden N, Whitesides GM. Angew Chem Int Ed 1999;38:3078–81.
[12] Elemans JAAW, Rowan AE, Nolte RJM. J Mater Chem 2003;13:2661–70.
[13] Keizer HM, Sijbesma RP. Chem Soc Rev 2005;34:226–34.
[14] Jenekhe SA, Chen XL. Science 1999;283:372–5.
[15] Qin L, Li H, Wu L, Qiu D, Zhang X, Shen J. Chem Lett 2003;32:390–1.
[16] Li H, Liu Q, Qin L, Xu M, Lin X, Yin S, et al. J Colloid Interface Sci 2005;289:488–97.
[17] Brunsveld L, Folmer BJB, Sijbesma RP, Meijier EW. Chem Rev 2001;101:4071–98.
[18] Kato T. Science 2002;295:2414–8.
[19] Ikkala O, Brinke GT. Science 2002;295:2407–9.

[20] Fenniri H, Deng B-L, Ribbe AE, Hallenga K, Jacob J, Thiyagarajan P. Proc Natl Acad Sci USA 2002;99:6487–92.
[21] Sijbesma RP, Beijer FH, Brunsveld L, Folmer BJB, Irschberg JHKK, Lange RFM, et al. Science 1997;278:1601–4.
[22] Brunsveld L, Vekemans JAJM, Hirschberg JHKK, Sijbesma RP, Meijer EW. Proc Natl Acad Sci USA 2002;99:4977–82.
[23] Fujita N, Yamashita T, Asai M, Shinkai S. Angew Chem Int Ed 2005;44: 1257–61.
[24] Duan HW, Chen DY, Jiang M, Guan WJ, Li SJ, Wang M, et al. J Am Chem Soc 2001;123:12097–8.
[25] Liu XY, Jiang M, Yang SL, Chen MQ, Chen DY, Yang C, et al. Angew Chem Int Ed 2002;41:2950–3.
[26] Hirst AR, Smith DK, Feiters MC, Geurts HPM, Wright AC. J Am Chem Soc 2003;125:9010–1.
[27] Li H, Liu Q, Xu M, Bu W, Lin X, Wu L, et al. J Phys Chem B 2005;109: 2855–61.
[28] Li H, Song B, Qin L, Liu Q, Wu L, Shen J. J Colloid Interface Sci 2005; 290:557–63.
[29] Price DJ, Willis K, Richardson T, Ungar G, Bruce W. J Mater Chem 1997;7:883–91.
[30] Percec V, Ahn C-H, Ungar G, Yearday DJP, Möller M, Sheiko SS. Nature 1998;391:161–4.
[31] Kato T, Fréchet JMJ. Macromolecules 1989;22:3818–9.
[32] Kato T, Fréchet JMJ, Wilson PG, Saito T, Uryu T, Fujishima A, et al. Chem Mater 1993;5:1094–100.
[33] Ajayaghosh A, Varghese R, Praveen VK, Mahesh S. Angew Chem Int Ed 2006;45:3261–4.
[34] Hoffmann H, Rehage H, Schorr W, Thurn H. In: Mittal KL, Lindman B, editors. Surfactants in solution, vol. 1. New York: Plenum Press; 1984.
[35] Ryu J-H, Lee M. J Am Chem Soc 2005;127:14170–1.
[36] Estroff LA, Hamilton AD. Chem Rev 2003;104:1201–17.
[37] Yang M, Wang W, Yuan F, Zhang X, Li J, Liang F, et al. J Am Chem Soc 2005;127:15107–11.
[38] Kim J-K, Hong M-K, Ahn J-H, Lee M. Angew Chem Int Ed 2005;44: 328–32.
[39] Cheng X, Huang Y, Tang R-P, Chen E, Xi F. Macromolecules 2005;38: 3044–7.
[40] Bae J, Choi J-H, Yoo Y-S, Oh N-K, Kim B-S, Lee M. J Am Chem Soc 2005;127:9668–9.
[41] Enomoto M, Kishimura A, Aida T. J Am Chem Soc 2001;123:5608–9.